

# Newtonian Flow Behavior of Hyperbranched High-Molecular-Weight Polyethylenes Produced with a Pd–Diimine Catalyst and Its Dependence on Chain Topology

Zhibin Ye and Shiping Zhu\*

Department of Chemical Engineering, McMaster University,  
1280 Main Street West, Hamilton,  
Ontario, Canada L8S 4L7

Received January 3, 2003

Revised Manuscript Received February 27, 2003

**Introduction.** Over the past two decades, dendritic polymers that include dendrimers and hyperbranched polymers have attracted great attention in research and development.<sup>1</sup> Compared to linear analogues, dendritic polymers have unique rheological properties in both solution and melt. The materials exhibit much lower viscosity than linear analogues and possess Newtonian flow behavior, i.e., no shear thinning or thickening due to lack of chain entanglements.<sup>2</sup> The surface congestion of the densely packed polymer molecules and highly branched chain topological structure are believed to be the major factors that prevent chain entanglements between polymer molecules.<sup>2a</sup>

Most reported dendritic polymers are made from condensation polymerization of AB<sub>x</sub>-type monomers and more recently through a “self-condensing” approach. The dendritic branch structure is introduced by incorporating specially designed type of monomers.<sup>1</sup> Recently, Guan et al.<sup>3</sup> reported a unique “chain walking” strategy to prepare hyperbranched polyethylenes by a coordination polymerization of ethylene with Pd–diimine catalysts, which were first developed by Brookhart et al.<sup>4</sup> Rather than introducing branches from monomer structure, the branching structure in this approach is introduced by the catalyst that controls the position for monomer addition.<sup>3a</sup> By coordinating the competition between chain walking and chain propagation through adjusting polymerization conditions, such as ethylene pressure and reaction temperature, a series of polyethylene grades with chain topology ranging from linear to moderately branched to hyperbranched samples can be generated.<sup>3,4</sup>

Strictly speaking, the hyperbranched polyethylenes produced in this approach have branching mechanism and structure different from those products made from AB<sub>x</sub> monomers.<sup>3b,e</sup> However, studies showed that, due to the branch-on-branch chain structure, the hyperbranched PEs produced at low ethylene pressure (0.1 atm) exhibited dilute solution properties observed for dendritic polymers.<sup>3,5</sup> From neutron scattering<sup>3d,5b</sup> and AFM studies,<sup>3e</sup> it was also found that these polymers resembled the compact globular structure observed in dendritic polymers. It is of fundamental importance and practical interest to further reveal the hyperbranch nature and rheological properties of these polyethylenes. This work reports the first rheological study on the flow behavior of this type of hyperbranched polymers and also investigates the effects of chain topology on the rheological properties.

**Experimental Section. a. Materials.** All manipulations with air- and/or moisture-sensitive compounds were carried out in a N<sub>2</sub>-filled drybox or using Schlenk

techniques. UHP N<sub>2</sub> (from Matheson Gas) and polymerization-grade ethylene (from Matheson Gas) were purified by passing through CuO, Ascarite, and 5A molecular sieves. Methanol, diethyl ether (anhydrous), CH<sub>2</sub>Cl<sub>2</sub> (anhydrous), cycloocta-1,5-diene (COD), Na<sub>2</sub>PdCl<sub>4</sub>, (CH<sub>3</sub>)<sub>4</sub>Sn, 2,6-diisopropylaniline, 2,3-butanediol, and AgSbF<sub>6</sub> were all purchased from Aldrich. The diimine ligand,<sup>6</sup> CODPdMeCl,<sup>7</sup> and Pd–diimine catalyst, [(ArN=C(Me)–C(Me)=NAr)Pd(CH<sub>3</sub>)(NCMe)]SbF<sub>6</sub> (Ar = 2,6-(*i*-Pr)<sub>2</sub>C<sub>6</sub>H<sub>3</sub>),<sup>8</sup> were synthesized according to the literature procedures.

**b. Polymer Synthesis.** The polymerization at ethylene pressure of 0.2 atm was conducted in a 500 mL glass reactor. A stock solution of catalyst in CH<sub>2</sub>Cl<sub>2</sub> was prepared. 100 mL of CH<sub>2</sub>Cl<sub>2</sub> was added to the flame-dried reactor under a N<sub>2</sub> atmosphere. The reactor was then sealed and heated to 35 °C with an oil bath, and the pressure inside was balanced to 0 atm (gauge). Subsequently, the reactor was pressurized with ethylene to 0.2 atm. After equilibrium for 10 min, the polymerization was started by injecting a certain amount of catalyst stock solution into the reactor. Ethylene pressure was kept constant at 0.2 atm throughout the reaction, and the temperature was maintained at 35 °C by the oil bath. After 20 h, the reactor was evacuated, and the mixture was added to a large amount of methanol. Then methanol was decanted off, the sticky polymer was redissolved in petroleum ether, and the solution was then filtered through a short plug of neutral alumina and silica. The petroleum ether in the filtered solution was then evaporated, and the viscous polymer oil was dried at 70 °C under vacuum for 1 week.

The polymerization at ethylene pressure of 1.0 atm followed a similar procedure. The glass reactor containing 100 mL of CH<sub>2</sub>Cl<sub>2</sub> was sealed, vacuumed, and then heated to the reaction temperature with an oil bath. The reactor was then pressurized with ethylene to 1.0 atm. Then after 10 min, a certain amount catalyst stock solution was injected. After a chosen period of reaction time as reported in Table 1, the reactor was vented. The reaction mixture was then added to a large amount of methanol. Subsequently, the solvent was decanted off, and the polymer was redissolved in petroleum ether. The polymer solution was filtered through alumina and silica to remove catalyst residues. Finally, the polymer was dried at 70 °C under vacuum for 1 week.

The polymerizations at 6.5 and 30 atm were carried out in a 1 L Autoclave stainless steel reactor. The reactor was carefully cleaned with acetone, heated to 140 °C under vacuum for 2 h, purged five times with UHP nitrogen, and then cooled to room temperature. 300 mL of CH<sub>2</sub>Cl<sub>2</sub> and a certain amount of catalyst stock solution were added into the reactor under nitrogen protection. The mixture was stirred for 10 min while being heated to the reaction temperature. The reactor was then pressurized to the desired ethylene pressure to start polymerization. The reactor temperature was controlled by flowing water through internal cooling coil of the reactor. The reaction was stopped by venting the reactor after a chosen period of time as shown in Table 1. The solvent in the mixture was evaporated, and sticky polymer sample was recovered and redissolved in petroleum ether. The polymer solution was filtered through alumina and silica to give a clear colorless

**Table 1. Polymerization Conditions and Polymer Properties<sup>a</sup>**

polymer	catalyst amount ( $\mu\text{mol}$ )	ethylene press. (atm)	temp ( $^{\circ}\text{C}$ )	time (h)	polymer produced (g)	$M_w^b$ (kg/mol)	PDI <sup>b</sup>	$[\eta]^b$ (dL/g)	$T_g^c$ ( $^{\circ}\text{C}$ )	$\eta_0^d$ (Pa s)	$E_a^e$ (kJ/mol)
1	200	0.2	35	20	6.3	94	2.3	0.093	-67	25	46.4
2	100	1.0	35	18	12.7	161	2.1	0.14	-65	43	43.8
3	100	1.0	25	18	27.3	149	2.2	0.35	-65	196	47.0
4	100	6.5	25	19	70.7	165	2.7	0.54	-64	$8.0 \times 10^4$	51.9
5	90	30.0	25	5	12.2	140	2.4	0.82	-63	$9.1 \times 10^4$	57.2

<sup>a</sup> Other reaction conditions: solvent 100 mL of  $\text{CH}_2\text{Cl}_2$  for polymers 1–3 and 300 mL of  $\text{CH}_2\text{Cl}_2$  for polymers 4 and 5. <sup>b</sup> From GPCV measurement at 140  $^{\circ}\text{C}$  in TCB. <sup>c</sup> From DSC measurement. <sup>d</sup> Polymer melt zero-shear viscosity at 25  $^{\circ}\text{C}$ , for polymers 4 and 5, the values calculated based on oscillation data using Cross equation. <sup>e</sup> Polymer melt flow activation energy calculated from the Arrhenius equation.

**Table 2. Polymer Short Chain Branching Distribution and Number of Branches per 1000 Carbons**

polymer	methyl	ethyl	propyl	butyl	pentyl	hexyl+	% <i>sec</i> -butyl <sup>a</sup>	total
1	35.7	26.2	2.8	12.1	3.1	40.1	23.7	118
2	33.7	24.2	2.4	11.5	2.9	37.2	23.5	112
3	32.9	23.8	2.2	11.4	2.7	37.7	23.4	111
4	33.0	23.1	3.1	11.3	3.1	35.5	20.0	109
5	32.0	19.3	3.5	9.4	3.5	34.2	16.6	102

<sup>a</sup> Percentage of methyl from *sec*-butyl branches in the total methyl branches. Measured by  $^{13}\text{C}$  NMR in  $\text{CDCl}_3$  at 30  $^{\circ}\text{C}$

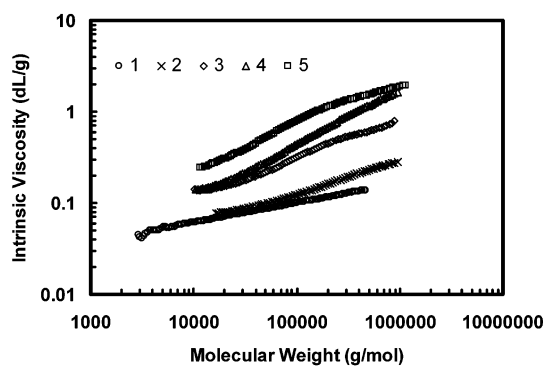
solution. The solvent was removed, and the sticky amorphous solid was dried at 70  $^{\circ}\text{C}$  under vacuum for 1 week.

**c. Polymer Characterization.** The glass transition temperatures were measured using a Thermal Analysis 2910 MDSC from TA Instruments in the standard DSC mode. UHP  $\text{N}_2$  gas at a flow rate of 30 mL/min was purged through the calorimeter. The temperature and heat capacity for the instrument were initially calibrated with indium standard at the heating rate of 10  $^{\circ}\text{C}/\text{min}$ . The polymer sample (about 20 mg) was first cooled to -120  $^{\circ}\text{C}$  with liquid nitrogen. It was then heated to 50  $^{\circ}\text{C}$  at 10  $^{\circ}\text{C}/\text{min}$ .

The polymer molecular weight (MW), molecular weight distribution (MWD), and intrinsic viscosity ( $[\eta]$ ) were measured at 140  $^{\circ}\text{C}$  in 1,2,4-trichlorobenzene using a Waters Alliance GPCV 2000 with DRI detector coupled with an in-line capillary viscometer. In the system, four Waters Styragel HT 6E linear columns were used. The flow rate was 1.0 mL/min, and the injection volume was 418.5  $\mu\text{L}$ . The concentrations of polymer solution were in the range 3–6 mg/mL. The data were collected every 0.1 s. The molecular weight was calculated according to a universal calibration curve based on 11 polystyrene narrow standards with molecular weight ranging from  $1.09 \times 10^6$  to 1000 g/mol.

The 75.4 MHz  $^{13}\text{C}$  NMR analysis was conducted on a Bruker AV300 pulsed NMR spectrometer with Waltz-supercycle proton decoupling at 30  $^{\circ}\text{C}$ . The polymer sample was dissolved in  $\text{CDCl}_3$  in 10 mm NMR tubes with concentration about 20 wt %. At least 4000 scans were applied for each acquisition to obtain a good signal-to-noise ratio.

All rheological characterizations of the polymer melts were conducted on a Stresstech HR rheometer in a 25 mm parallel plate mode with a gap of 1.0 mm. The instrument was calibrated with 1000 cP standard oil. The experiments were performed at regular 5  $^{\circ}\text{C}$  intervals within temperature range from 25 to 65  $^{\circ}\text{C}$  and at 10  $^{\circ}\text{C}$  intervals within temperature range from 65 to 115  $^{\circ}\text{C}$ . The temperature was maintained within  $\pm 0.2$   $^{\circ}\text{C}$  using an ETC-3 temperature control system, and the measurements were done under a  $\text{N}_2$  blanket. The polymer samples were subject to steady shear, creep recovery, and small-amplitude dynamic oscillation in the controlled-stress mode. In the steady-shear mode, at least 3 orders of magnitude of shear rates was covered.

**Figure 1.** Intrinsic viscosity  $[\eta]$  as a function of MW in TCB at 140  $^{\circ}\text{C}$  from GPCV characterization.

In the creep recovery experiments, the samples were subject to stress at time zero, and the compliance was monitored at constant stress for 200 s, at which time the applied stress was removed, and the relaxation behavior was recorded. This procedure was then repeated with different stresses. In the small-amplitude dynamic oscillation mode, the frequency range covered 0.001 to 90 Hz. Strain sweeps were performed before frequency sweeps to establish the linear viscoelastic region. All the three measurements were conducted on the same loaded sample. At the end of the experiments, the sample was retested at 25  $^{\circ}\text{C}$  to confirm the stability of the sample during measurement. For all the samples, this difference did not exceed  $\pm 5\%$ .

**Results and Discussion.** A series of polymer samples with different chain topologies were synthesized in this work with  $[(\text{ArN}=\text{C}(\text{Me})-\text{C}(\text{Me})=\text{NAr})\text{Pd}(\text{CH}_3)(\text{NCMe})]\text{-SbF}_6$  ( $\text{Ar} = 2,6\text{-(iPr)}_2\text{C}_6\text{H}_3$ ) as catalyst under various reaction conditions. Table 1 summarizes the reaction conditions and polymer properties measured by DSC, GPCV, and rheometry. Table 2 presents the short chain branch distributions for these polymers. Similar to those reported by Brookhart et al.<sup>9</sup> and Guan et al.,<sup>3</sup> these polymers showed little change in total branch and short chain distribution. The polymers had high molecular weights. Their average molecular weights and polydispersities were quite close. However, as reported by Guan et al.,<sup>3</sup> a significant difference in the intrinsic viscosities was observed. Figure 1 shows the dependence of  $[\eta]$  on MW for the five samples characterized by GPCV. Increasing the reaction pressure from 0.2 to 30 atm and

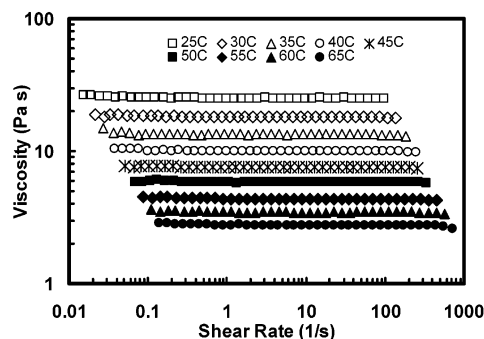


**Figure 2.** Steady-shear viscosity as a function of shear rate for polymer 1 measured at various temperatures.

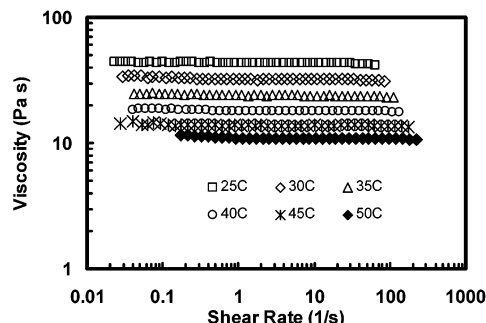


**Figure 3.** Steady-shear viscosity as a function of shear rate for polymer 2 measured at various temperatures.

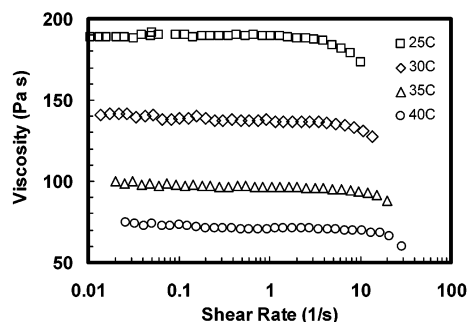


**Figure 4.** Steady-shear viscosity as a function of shear rate for polymer 3 measured at various temperatures.

decreasing the reaction temperature from 35 to 25 °C significantly increased the intrinsic viscosities at the same molecular weight, suggesting the change of chain topology from hyperbranched to a relatively linear structure.

Figures 2 and 3 show the melt viscosity curves for polymers 1 and 2, respectively, from steady-shear measurements, which were conducted in a broad range of shear rates and at various temperatures. The two polymers, synthesized at low ethylene pressures (0.2 and 1.0 atm, respectively) and 35 °C, were viscous oil-like. These polymers exhibited a Newtonian flow behavior typical of hyperbranched polymers, i.e., the independence of viscosity on shear rate. The dynamic oscillation tests were also performed in the linear viscoelastic region. Typically Figure 5 shows the complex viscosity measured at 25 °C vs oscillation frequency. The complex viscosities equaled their corresponding steady-shear values and were also independent of frequency at all the temperatures tested. In the creep-recovery experiments, these two polymers showed ideal viscous behavior in the range of applied stresses and temperatures. All these rheological results suggest that these highly branched high-molecular-weight oils mimic

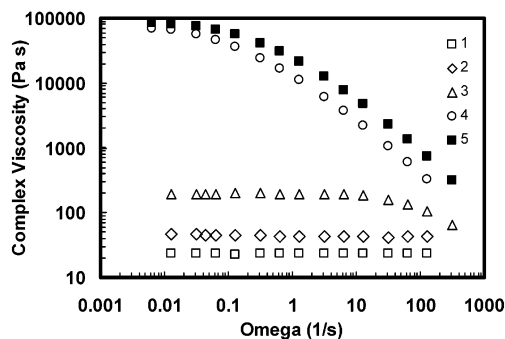


**Figure 5.** Complex viscosity as a function of frequency from oscillation measurements at 25 °C.

the characteristic rheological properties typical of hyperbranched polymers, i.e., the absence of chain entanglements.

In the work by Guan et al.,<sup>3</sup> a series of highly branched polyethylenes were also synthesized by a similar Pd–diimine catalyst,  $[(\text{ArN}=\text{C}(\text{Me})-\text{C}(\text{Me})=\text{NAr})\text{Pd}(\text{CH}_2)_3\text{C}(\text{O})\text{OMe}]\text{BAF}$  ( $\text{Ar} = 2,6\text{-}(\text{iPr})_2\text{C}_6\text{H}_3$ ), at similar reaction conditions. On the basis of the ratio of  $R_g$  (gyration radius) and  $R_H$  (hydrodynamic radius) ( $R_g/R_H < 1$ ) from light scattering measurements and on the neutron scattering behavior (a maximum in the Kratky plot), they found that at reaction temperature of 35 °C only those polymer samples produced at very low ethylene pressure (0.1 atm) exhibited topology nature similar to dendritic polymers. However, from the rheological measurements, this work showed that at this reaction temperature, the polymers produced at even higher pressures (0.2 and 1 atm) resembled dendritic polymers. This difference might be due to the fact that the  $R_g/R_H$  ratio and neutron scattering behavior are less sensitive toward branching structure than melt rheological behavior. It might also be because of the different catalysts used in the polymerizations, which caused a difference in the polymer structure, such as molecular weight and branch structure.

Elevating the pressure and/or lowering the reaction temperature to 25 °C during polymerization yielded a viscous sticky oil (polymer 3) and sticky elastic solids (polymers 4 and 5). In contrast to the Newtonian flow behavior observed in polymers 1 and 2, shear thinning behaviors were observed for these three samples from both steady-shear and dynamic oscillation measurements. Figure 4 shows the steady-shear viscosity vs shear rate for polymer 3 at different measurement temperatures. Different from Figures 2 and 3, an obvious decrease of viscosity at high shear rate end can be observed. Moreover, in Figure 5, the different dependences of complex viscosity on oscillation frequency for the five polymers at 25 °C were compared. The complex viscosity for polymers 1 and 2 is independent of the oscillation frequency. However, for polymers 3–5, increasing the oscillation frequency significantly decreased the complex viscosity, suggesting relatively linear chain topology and presence of chain entanglements in these polymers. More importantly, compared to polymer 3, polymers 4 and 5 exhibited more pronounced shear thinning, showing the more chain entanglements involved in the polymers having more linear chain topology.

The zero-shear viscosities at 25 °C for these five polymers, which exhibit very close average molecular weight, are summarized in Table 1. Changing the chain topology from hyperbranched to linear structure in-



creased the viscosity dramatically (more than 3 orders of magnitude). The effects of temperature on the rheological properties of the five samples all agreed with the Arrhenius equation in the temperature range. Despite their non-Newtonian flow behavior, polymers 3–5 exhibited simple thermal rheological behavior. The flow activation energies were calculated on the basis of the time–temperature supposition and were reported in Table 1. Compared to HDPE ( $E_a = 27$  kJ/mol) and LLDPE ( $E_a \approx 34$  kJ/mol),<sup>10</sup> these highly branched polymers had enhanced flow activation energy ( $E_a = 44$ –57 kJ/mol). The flow activation energy tends to increase when the chain topology changes from a hyperbranched to linear structure.

**Conclusion.** This work examined the rheological properties for a series of highly branched polyethylene samples prepared with a Pd–diimine catalyst system. It was revealed that the polymers produced at low pressure (0.2 and 1 atm) and higher temperature (35 °C) exhibited rheological behavior characteristic of hyperbranched polymers. The samples had very low viscosities and showed Newtonian flow behavior due to the absence of chain entanglements. The change of chain topology from hyperbranched to linear led to much higher viscosity and non-Newtonian flow behavior due to chain entanglements.

**Acknowledgment.** The authors appreciate the Ministry of Education, Science and Technology of Ontario for a PREA award. Z.Y. also thanks the Ministry for an Ontario Graduate Scholarship (OGS).

## References and Notes

- (1) (a) Fréchet, J. M. J. *J. Macromol. Sci., Pure Appl. Chem.* **1996**, A33, 1399. (b) Newkome, G. R. *Advances in Dendritic Macromolecules*; JAI Press: Greenwich, CT, 1993. (c) Roovers, J.; Comanita, B. *Adv. Polym. Sci.* **1999**, 142, 179. (d) Fischer, M.; Vögtle, F. *Angew. Chem., Int. Ed.* **1999**, 38, 884. (e) Hult,

- A.; Johansson, M.; Malmström, E. *Adv. Polym. Sci.* **1999**, 143, 1.
- (2) (a) Hawker, C. J.; Farrington, P. J.; Mackay, M. E.; Wooley, K. L.; Fréchet, J. M. J. *J. Am. Chem. Soc.* **1995**, 117, 4409. (b) Uppuluri, S.; Keinath, S. E.; Tomalia, D. A.; Dvornic, P. R. *Macromolecules* **1998**, 31, 4498. (c) Jahromi, S.; Palmen, J. H. M.; Steeman, P. A. M. *Macromolecules* **2000**, 33, 577. (d) Scherrenberg, R.; Coussens, B.; van Vliet, P.; Edouard, G.; Brackman, J.; de Brabander, E. *Macromolecules* **1998**, 31, 456. (e) Sendijarevic, I.; McHugh, A. J. *Macromolecules* **2000**, 33, 590. (f) Nunez, C. M.; Chiou, B.-S.; Andrad, A. L.; Khan, S. A. *Macromolecules* **2000**, 33, 1720. (g) Suneel, D.; Buzza, M. A.; Groves, D. J.; McLeish, T. C. B.; Parker, D.; Keeney, A. J.; Feast, W. J. *Macromolecules* **2002**, 35, 9605.
- (3) (a) Guan, Z.; Cotts, P. M.; McCord, E. F.; McLain, S. J. *Science* **1999**, 283, 2059. (b) Cotts, P. M.; Guan, Z.; McCord, E.; McLain, S. *Macromolecules* **2000**, 33, 6945. (c) Guan, Z.; Cotts, P. M.; McCord, E. F. *Polym. Prepr.* **1998**, 39, 402. (d) Guan, Z.; Cotts, P. M. *Polym. Mater. Sci. Eng.* **2001**, 84, 382. (e) Guan, Z. *Chem.-Eur. J.* **2002**, 8, 3086.
- (4) (a) Ittel, S. D.; Johnson, L. K.; Brookhart, M. *Chem. Rev.* **2000**, 100, 1169. (b) Johnson, L. K.; Killian, C. M.; Brookhart, M. *J. Am. Chem. Soc.* **1995**, 117, 6414. (c) Tempel, D. J.; Johnson, L. K.; Huff, R. L.; White, P. S.; Brookhart, M. *J. Am. Chem. Soc.* **2000**, 122, 6686.
- (5) (a) Plentz Meneghetti, S.; Kress, J.; Lutz, P. J. *Macromol. Chem. Phys.* **2000**, 201, 1823. (b) Lutz, P. J.; Plentz, Meneghetti, S.; Kress, J.; Lapp, A.; Duval, M. *Polym. Prepr.* **2000**, 41, 1882.
- (6) tom Dieck, H.; Svoboda, M.; Grieser, T. Z. *Naturforsch.* **1981**, 35b, 823.
- (7) (a) Chatt, J.; Vallarino, L. M.; Venanzi, L. M. *J. Chem. Soc.* **1957**, 3413. (b) Rülke, R. E.; Ernsting, J. M.; Spek, A. L.; Elsevier, C. J.; van Leeuwen, P. W. N. M.; Vrieze, K. *Inorg. Chem.* **1993**, 32, 5769.
- (8) Mecking, S.; Johnson, L. K.; Wang, L.; Brookhart, M. *J. Am. Chem. Soc.* **1998**, 120, 888.
- (9) McLain, S. J.; McCord, E. F.; Johnson, L. K.; Ittel, S. D.; Nelson, L. T. J.; Arthur, S. D.; Halfhill, M. J.; Teasley, M. F.; Tempel, D. J.; Killian, C.; Brookhart, M. S. *Polym. Prepr.* **1997**, 38, 772.
- (10) Malmberg, A.; Kokko, E.; Lehmus, P.; Löfgren, B. Seppälä, J. V. *Macromolecules* **1998**, 31, 8448.

MA0340053